

Johanna Mazlo,^a Robyn L. Stanfield,^b Ian A. Wilson,^b Steven H. Hinrichs^{c,d,*} and John J. Stezowski^a

^aDepartment of Chemistry, University of Nebraska-Lincoln, Lincoln, NE 68588-0304, USA, ^bThe Scripps Research Institute, La Jolla, CA 92037, USA, ^cDepartment of Pathology and Microbiology, University of Nebraska Medical Center, Omaha, NE 68198, USA, and ^dEppley Institute for Research in Cancer and Allied Diseases, University of Nebraska Medical Center, Omaha, NE 68198, USA

Correspondence e-mail: shinrich@unmc.edu

Preliminary X-ray diffraction studies of the transcriptional inhibitory antibody Fab41.4

The binding of transcription factor ATF-1 to DNA contributes to gene expression and regulation of cell growth. Antibody Mab41.4, raised against ATF-1, and its derivatives Fab41.4 and scFv41.4 inhibit specific DNA binding *in vitro* and induce apoptotic death of tumor cells *in vivo*. Structural studies of Fab41.4 were performed to gain insight into the mechanism of action of this potentially therapeutic antibody. The optimal conditions for crystallization of Fab41.4 were determined. Crystals were needle-like in appearance, displayed C2 space-group symmetry and diffracted to a resolution of 1.6 Å. The unit-cell parameters were determined to be $a = 186.64$, $b = 40.22$, $c = 55.58$ Å, $\alpha = \gamma = 90$, $\beta = 96.93^\circ$. The data set was 97.7% complete. Molecular replacement was performed, resulting in an R value of 44.6%.

Received 27 October 2000
Accepted 16 January 2001

1. Introduction

Activating transcription factor-1 (ATF-1) is a member of the large bZIP family of transcription factors. The defining features of the bZIP superfamily include a DNA-binding region containing basic amino-acid residues (b) and a dimerization domain containing heptad repeats of leucine, the leucine zipper (ZIP). ATF-1 binds as a homodimer to DNA, with each monomer having a molecular weight of 36 000 Da. As a member of the CREB/ATF subfamily, ATF-1 binds to a cAMP response element (CRE), with the consensus sequence being an eight base-pair palindrome 5'-TGACGTCA-3' (Lee & Masson, 1993). ATF-1 binds with high affinity to the CRE sequence and with considerably lower affinity to DNA sequences that are similar, such as the AP-1 site (TGAGTCA; Bosilevac *et al.*, 1998). The specific role of ATF-1 in normal cells is unknown; however, a chimeric protein resulting from chromosomal translocation of the ATF-1 DNA-binding domain is associated with the development of a specific type of cancer termed clear-cell sarcoma (Travis & Bridge, 1992). Further, ATF-1 is expressed at significantly lower levels in differentiated cells compared with undifferentiated cells, but is overexpressed in continuously proliferating cells such as HeLa cells (Masson *et al.*, 1993). A recent study has suggested that ATF-1 is also a survival factor for human melanoma cells (Jean *et al.*, 2000).

X-ray diffraction studies have been reported for the prototypic bZIP yeast transcription factor GCN4 bound to AP-1 (O'Shea *et al.*, 1991) and CRE DNA (Ellenberger *et al.*, 1992;

Konig & Richmond, 1993). The DNA-binding domain of GCN4 consists of basic residues, with a conserved asparagine contacting the cytosine and thymidine within one half-site of a CRE and a conserved arginine binding to the cytosine and guanine of the second CRE half-site (Konig & Richmond, 1993). The α -helix of GCN4 resided in the major groove; however, no electron-density assignment was possible beyond the DNA-binding domain. ATF-1 interactions with CRE DNA are expected to be similar to those of GCN4.

Mab41.4 (IgG1, κ) is one of a group of ATF-1-specific antibodies that were obtained through use of recombinant ATF-1 as an immunogen (Orten *et al.*, 1994). Mab41.4 was found to inhibit ATF-1/DNA binding *in vitro* (Gilchrist *et al.*, 1995) and in cells (Bosilevac *et al.*, 1998). Recently, the expression of scFv41.4 in MeWo melanoma cells suppressed tumor growth and induced apoptosis *in vivo* (Jean *et al.*, 2000). The Fab of Mab41.4 contains the V_L, C_L, V_H and C_H1 regions, which incorporate the antigen-binding portions. In addition, recombinant scFv has been cloned (Bosilevac *et al.*, 1998) and, when expressed in cells, retained the inhibitory activity of the parent antibody (Bosilevac *et al.*, 1999). scFv41.4 contains the V_H and V_L regions of Mab41.4, with a 15 amino-acid linker inserted between the heavy and light variable regions. The epitope of antibody 41.4 has been mapped and is represented by a 15 amino-acid sequence, Peptide C. Since scFv41.4 retains the inhibitory activity *in vivo*, a structural analysis of its interactions is important for guiding future refinements. Information regarding its structure is expected to aid in the development of Fab41.4 analogs

that may have greater affinity or specificity for further experimental studies and therapeutic applications.

2. Methods and materials

Mab41.4 was obtained from ascites fluid as described by Orten *et al.* (1994). Fab41.4 was obtained from Mab41.4 by papain digestion. Protein A column separation was used to purify the Fab41.4 from the Fc41.4 fragments and undigested Mab41.4. The Fab41.4 elution buffer was 3 M NaCl/1.5 M glycine pH 8.9 (Gilchrist *et al.*, 1995). The Fab41.4 was dialyzed into PBS and separated by SDS-PAGE to determine the purity of the product.

The preliminary crystallization experiments were carried out using the vapor-diffusion method and various crystal screens. Crystals were obtained with the Hampton Crystal Screen I (Cudney *et al.*, 1994). By adjusting the percentage of PEG, higher quality crystals were generated. Subsequent fine screening identified the optimal crystallization conditions to be 22% PEG 8000, 0.1 M sodium cacodylate pH 6.5, 0.2 M magnesium acetate and 10% glycerol. A drop consisted of 3 μ l 10 mg ml⁻¹ Fab41.4 mixed with 3 μ l of the reservoir solution.

Data collection was carried out on station BL7-1 at the Stanford Synchrotron Radiation Laboratory (SSRL) using a 345 mm

MAR Research image plate and radiation of wavelength 1.08 Å. The crystallization buffer performed as a cryobuffer that allowed the crystals to be cryocooled by rapid transfer to a nitrogen-gas stream at 100 K.

The data were reduced and the unit-cell parameters were deduced using the *HKL* software (Otwinoski & Minor, 1997). The structure of Fab41.4 was solved using molecular replacement with the evolutionary search algorithm of the *EPMR* program (Kissinger *et al.*, 1999). Fab44.1 (IgG1_K; PDB file 1mlc) was selected as an initial model because it produced the best results compared with the other Fabs that were examined using *EMPR*. A homology search using the variable-region sequence against the antibody database at Scripps was performed. The V_L region and the V_H region were replaced with the most homologous crystallized antibodies. The rigid-body refinement from *CNS* (Brunger *et al.*, 1998) was applied using four domains: V_L, C_L, V_H and C_H1.

3. Results and discussion

Crystal formation occurred within one week of setup at room temperature. Typically, needle-like crystals with several branching sites were observed. The microseeding technique yielded the most useful crystals for X-ray analysis. (Fitzgerald & Madsen, 1986). Setups used 1 μ l of microseeds derived from the branched needle crystals added to the drop. Long needle-shaped single crystals appeared with typical dimensions of 1 \times 0.5 \times 0.2 mm. Data were collected from crystals of Fab41.4 alone. Data conformed to a space-group symmetry of C2, with unit-cell parameters $a = 186.64$, $b = 40.23$, $c = 55.58$ Å, $\alpha = \gamma = 90$, $\beta = 96.93^\circ$. The crystal diffracted to a resolution of 1.6 Å. Assuming the molecular weight of Fab41.4 to be 50 kDa and one Fab41.4 per asymmetric unit, the respective volume per unit molecular weight (V_M) was 2.17 Å³ Da⁻¹ (Matthews, 1968).

The data set from a crystal of Fab41.4 was 97.7% complete (Table 1). Molecular replacement using the evolutionary search algorithm of the *EPMR* program was carried out. First, molecular replacement of the variable region was performed with Fab44.1, yielding a best correlation coefficient of 23%, with a 5% decrease in the second best result. The constant region then underwent molecular replacement resulting in a correlation coefficient of 43% and an *R* value of 47.7%. Subsequently, a variable-region homology search identified two antibodies

Table 1

Data-collection statistics.

Values in parentheses are for the highest resolution shell.	
Space group	C2
Unit-cell parameters (Å, °)	$a = 186.64$, $b = 40.23$, $c = 55.58$, $\beta = 96.93$
Resolution limits (Å)	27.6–1.6 (1.63–1.60)
Data-set completeness (%)	97.7 (96.0)
Total No. of reflections	193925 (8210)
No. of unique reflections	53192 (2575)
R_{sym} (%)	5.6 (63.2)
$I/\sigma(I)$	25.7 (2.32)

with a higher sequence homology than Fab44.1, including Fab58.2 and MOPC21. The V_L region was replaced with the coordinates of Fab58.2 (PDB file 1f58) and the V_H region was replaced with MOPC21 (PDB file 1igl) (Fig. 1). Using *CNS*, a rigid-body refinement of the four domains V_L, C_L, V_H and C_H1 yielded an *R* value of 44.6% and an R_{free} (containing 5% of the data) of 47.3%. Current efforts are focused on determining the structure of the complementarity-determining regions of Fab41.4.

We are grateful to Cindy A. Gilchrist and Kathy M. Selbo for technical support. We also thank Tzanko I. Doukov for assistance with data collection. This work is based upon research conducted at the Stanford Synchrotron Radiation Laboratory (SSRL), which is funded by the Department of Energy (BES, BER) and the National Institutes of Health (NCRR, NIGMS). This work was supported in part by State of Nebraska LB595 Cancer and Smoking Disease Research Grant to the UNMC Eppley Cancer Center and the Warren F. and Edith R. Day Student Aid Fund Award.

References

- Bosilevac, J. M., Gilchrist, C. A., Jankowski, P. E., Paul, S., Rees, A. R. & Hinrichs, S. H. (1998). *J. Biol. Chem.* **273**, 16874–16879.
- Bosilevac, J. M., Olsen, R. J., Bridge, J. A. & Hinrichs, S. H. (1999). *J. Biol. Chem.* **274**, 34811–34818.
- Brunger, A. T., Adams, P. D., Clore, G. M., DeLano, W. L., Gros, P., Grosse-Kunstleve, R. W., Jiang, J. S., Kuszewski, J., Nilges, M., Pannu, N. S., Read, R. J., Rice, L. M., Simonson, T. & Warren, G. L. (1998). *Acta Cryst.* **D54**, 905–921.
- Cudney, R., Patel, S., Weisgraber, K., Newhouse, Y. & McPherson, A. (1994). *Acta Cryst.* **D50**, 414–423.
- Ellenberger, T. E., Brandl, C. J., Struhl, K. & Harrison, S. C. (1992). *Cell*, **71**, 1223–1227.
- Fitzgerald, P. M. D. & Madsen, N. B. (1986). *J. Cryst. Growth*, **76**, 600–606.
- Gilchrist, C. A., Orten, D. J., Bosilevac, J. M., Sanderson, D. S. & Hinrichs, S. H. (1995). *Antibody Immunconjugates Radiopharm.* **8**, 281–298.

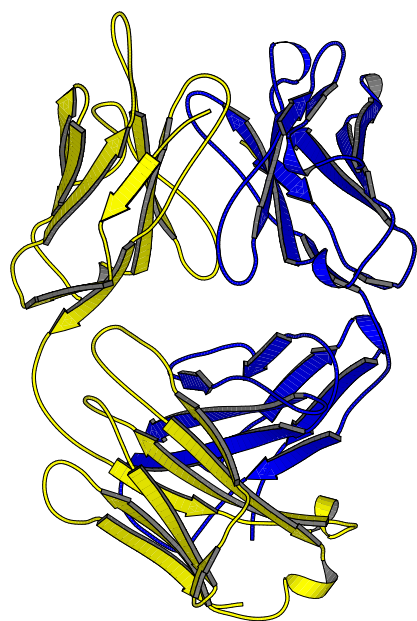


Figure 1

Representation of Fab41.4 following molecular replacement. The V_L region was replaced with the coordinates of Fab58.2 and the V_H region was replaced with MOPC21.

- Jean, D., Tellex, C., Huang, S., Davis, D. W., Bruns, C. J., McConkey, D. J., Hinrichs, S. H. & Bar-Eli, M. (2000). *Oncology*, **19**, 2721–2730.
- Kissinger, C. R., Gehlhaar, D. K. & Fogel, D. B. (1999). *Acta Cryst. D* **55**, 484–491.
- Konig, P. & Richmond, T. J. (1993). *J. Mol. Biol.* **233**, 139–154.
- Lee, K. A. W. & Masson, N. (1993). *Biochim. Biophys. Acta*, **1174**, 221–233.
- Masson, N., Hurst, H. C. & Lee, K. A. W. (1993). *Nucleic Acids Res.* **21**, 1163–1169.
- Matthews, B. W. (1968). *J. Mol. Biol.* **33**, 491–497.
- Orten, D. J., Strawhecker, J. M., Sanderson, S. D., Huang, D., Prystowsky, M. B. & Hinrichs, S. H. (1994). *J. Biol. Chem.* **269**(51), 32254–32263.
- O’Shea, E. K., Klemm, J. D., Kim, P. S. & Alber, T. (1991). *Science*, **254**, 539–544.
- Otwinoski, Z. & Minor, W. (1997). *Methods Enzymol.* **276**, 307–326.
- Travis, J. A. & Bridge, J. A. (1992). *Cancer Genet. Cytogenet.* **64**, 104–106.